

Rotational friction on small globular proteins: Combined dielectric and hydrodynamic effect

Arnab Mukherjee and Biman Bagchi *

Solid State and Structural Chemistry Unit, Indian Institute of Science, Bangalore, India 560 012.

Abstract

Rotational friction on proteins and macromolecules is known to derive contributions from at least two distinct sources – hydrodynamic (due to viscosity) and dielectric friction (due to polar interactions). In the existing theoretical approaches, the effect of the latter is taken into account in an *ad hoc* manner, by increasing the size of the protein with the addition of a hydration layer. Here we calculate the rotational dielectric friction on a protein (ζ_{DF}) by using a generalized arbitrary charge distribution model (where the charges are obtained from quantum chemical calculation) and the hydrodynamic friction with stick boundary condition, (ζ_{hyd}^{stick}) by using the sophisticated theoretical technique known as tri-axial ellipsoidal method, formulated by Harding [S. E. Harding, *Comp. Biol. Med.* **12**, 75 (1982)]. The calculation of hydrodynamic friction is done with only the dry volume of the protein (no hydration layer). We find that the total friction obtained by summing up ζ_{DF} and ζ_{hyd}^{stick} gives reasonable agreement with the experimental results, i.e., $\zeta_{exp} \approx \zeta_{DF} + \zeta_{hyd}^{stick}$.

*Email: bbagchi@sscu.iisc.ernet.in

1 Introduction

In this article, we present an interesting result that the experimentally observed rotational correlation time of a large number of proteins can essentially be described as the combined effect of the rotational dielectric and hydrodynamic frictions on the proteins. Thus, one needs not assume the existence of a rigid hydration layer around the protein, as is often assumed in the standard theoretical calculations of hydrodynamic friction.

The study of rotational friction of proteins in aqueous solution has a long history [1 – 12]. Despite many decades of study, several aspects of the problem remain ill understood. For proteins and macromolecules, the rotational friction is obtained from Debye-Stokes-Einstein (DSE) relation given by,

$$\zeta_R = 8\pi\eta R^3, \quad (1)$$

where ζ_R is the rotational friction on the protein and R is the radius of the protein. Naturally, the above relation assumes a spherical shape of the protein, which is often not correct. Moreover, there is ambiguity about the determination of some average radius of the protein. If one obtains the radius from the standard mass density of the protein (0.73 gm/cc), the values of the rotational friction are much smaller. The dielectric measurement of Grant [4] showed that the experimental value of rotational friction of myoglobin could only be explained by the above DSE equation, if one assumes a thick hydration layer around the protein, thereby increasing the radius of the protein. It is well known that spherical approximation embedded in DSE is grossly in error and the shape of the protein is quite important. However, even with the more recent sophisticated techniques such as tri-axial ellipsoid method [5] and the microscopic bead modeling technique [6, 7], which take due recognition of the non-spherical shape of the macromolecule, agreement with the experimental result is not possible without the incorporation of a rigid hydration layer [10]. It should be recognized that the effect of hydration layer thus introduced is purely *ad hoc*. In the case of tri-axial ellipsoidal method, the values of the axes are

increased proportionately by increasing the percentage of encapsulation of the protein atoms inside its equivalent ellipsoid [11, 12]. On the other hand, the microscopic bead modeling technique uses beads of much bigger size [6] (3.0 \AA instead of 1.2 \AA) to take care of the effect of hydration layer. Without the hydration layer, the estimate of friction obtained from the theory is systematically lower.

It has been recognized quite early that water in the hydration layer surrounding proteins and macromolecules has completely different dynamical properties than those in the bulk [13]. The dynamics of water molecules in the hydration layer are also subject of great interest as they could play crucial role in the property and activity of these molecules. One often discusses the crossover from biological activity to the observed inactivity at low temperatures in terms of a protein-glass transition observed in the hydrated proteins [14]. Recent investigations have shown that the water molecules in the hydration layer are not only more structured but they also show slow translational and rotational motion than their bulk counterpart [15, 16, 17, 18, 19].

Nevertheless, it is highly unlikely that water molecules in the surface of a protein such as myoglobin are so slow that we can replace it by a rigid hydration layer. On the contrary, all the recent experimental and simulation studies have shown that the water in the surface of the protein exhibits bimodal dynamics [20]. Majority of the water molecules seem to retain their bulk-like dynamics while a fraction ($\sim 20\%$) exhibits markedly slow dynamics. Recent solvation dynamics and photon echo peak shift experiment not only established the existence of slow water on the surface of proteins but also showed that the hydration layer is quite labile [21]. If one defines an average residence time to characterize the dynamics of water in the hydration layer, the residence time of bound or quasi-bound water is expected to range from 20 to 300 ps [22]. Question naturally arises how to understand quantitatively the role of the hydration layer in enhancing the rotational friction on the protein molecules. Clearly, the picturesque description of an immobile rigid layer around protein needs to be replaced by a description where the hydration layer is slow but definitely

dynamic.

This labile hydration layer has been explained in terms of a dynamic exchange model, which assumes that due to the presence of relatively stronger hydrogen bonding of water molecules with the charged groups at the surface of the protein, a surface water molecule can exist in either of the following two states – bound and free [23]. The free water molecules have dynamical characteristics similar to those of the bulk but the bound water molecules are essentially made static by the hydrogen bonding with the surface. In this picture, the slow time scale arises due to the dynamical exchange between the two states of the water molecules. Recent computer simulations seem to have confirmed the essential aspects of the dynamic exchange model (DEM) [24].

While the above model can provide a simple explanation of the origin of the observed slow dynamics, its correlation with dynamical properties of protein has not yet been established. This is a non-trivial problem as discussed below.

The mode coupling theory (MCT) is another viable quantitative theory, which has been quite successful in describing translational and rotational motion of small molecules [25]. This approach has also been extended to treat dynamics of polymer and biomolecules [26]. Let us recall a few of the lessons learned from the MCT of rotational friction of small molecules, and translational friction of ions in dipolar liquids. In both the cases, intermolecular dipole-dipole/ion-dipole correlations were found to play important role. It was also found that if one neglects the translational mode of the solvent molecules, then the friction on polar solute increases by several factors. It should be noted here that the continuum models/hydrodynamic description of rotational friction always ignored this translational component. In fact, this translational component plays a hidden role in reducing the effect of the role of molecular level solute solvent and solvent-solvent pair (both isotropic and orientational) correlations that increase the value of the friction over the continuum model prediction. Thus, the issue is rather involved. In fact, the continuum model is found to give ac-

curate results due to cancellation of two errors: neglect of short-range correlations and neglect of translational contribution. In view of the above, it is thus important to note that the slow water molecules in the hydration layer can enhance the friction considerably. Thus, the classical picture of rigid, static hydration layer needs to be replaced by dynamic layer where the translational motion of the water molecules should be related to the residence time. However, only preliminary progress has been made in this direction. Thus, continuum models remain the only theoretical method to treat dielectric friction on complex molecules.

An important issue in the calculation of the rotational friction is that proteins are characterized by complex charge distribution. The earliest models to estimate the enhanced friction on a probe, due to the interactions of its polar groups with the surrounding water molecules in an aqueous solution, employed a point dipole approximation [27, 28, 29]. In the simplest version of the model, the probe molecule is replaced by a sphere with a point dipole at the *center* of the sphere. Such an approach is reasonable for small molecules, although continuum model itself may have certain limitations. The situation is quite different for large molecules like proteins because the charge here is distributed over a large volume and the surface charges are close to the water molecules. Thus, the point dipole approximation becomes inapplicable to such systems. This limitation of the early continuum models was removed by Alavi and Waldeck [30] who obtained an elegant expression for the dielectric friction on a molecule with extended arbitrary charge distribution. By studying several well-known dye molecules, they demonstrated that the extended charge distribution indeed has a strong effect on the dielectric friction on the probe molecules. The work of Alavi and Waldeck [30] constitutes an important advance in the study of dielectric friction. The role of dielectric friction has been studied for the organic molecules by other authors [31].

The objective of the present work is to attempt to replace the rigid hydration layer used in hydrodynamic calculation. To this goal, we

calculate the hydrodynamic friction using the tri-axial method [5], in which the shape of a protein is mapped to an ellipsoid of three unequal axes – closely representing the shape and size of the protein. No hydration layer is added in the calculation. We then calculate the dielectric friction using Alavi and Waldeck’s model of generalized charge distribution for a large number of proteins. The friction contributions obtained from the above two methods are combined to obtain the total rotational friction. When compared, the total friction has been found to agree closely with the experimental result.

We have also extended the work of Alavi and Waldeck to include multiple shells of water with different dielectric constants around a protein. The multiple shell model is introduced in concern with the experimental observation of varying dielectric constants of water from the hydration layer surrounding a protein to the bulk water. These shells have distinct dielectric properties – both static and dynamic. The resulting analytical expressions can be used to obtain quantitative prediction of the effects of a slow layer of water molecules on the dielectric friction on proteins. However, the multiple shell model in the continuum fails since it adds up the friction in every layer. This has been discussed in the appendix.

2 Results and Discussion

Below, we discuss the results obtained from the different aspects of rotational friction of proteins. The coordinates of the proteins are obtained from protein data bank (PDB) [32].

2.1 Dielectric Friction

Dielectric friction is an important part of rotational friction for polar or charged molecules in polar solvent, because of the polarization of the

solvent medium. The solvent molecules, being polarized by the probe, create a reaction field, which opposes the rotation of the probe.

Many of the amino acid residues, which constitute the protein, are polar or hydrophilic. Therefore, in the aqueous solution, a protein and other polar molecules experience significant dielectric friction. There exist several theories [27, 28, 29, 33, 34, 35], which account for the dielectric contribution to the friction. Some of these theories are continuum model calculation of a point charge or point dipole rotating within the spherical cavity. Nee and Zwanzig [27] provide an estimate of dielectric friction on a point dipole in terms of the dipole moment of the point dipole, dielectric constant of the solvent, Debye relaxation time, and the chosen cavity radius. Later, Alavi and Waldeck [30] extended this theory to incorporate the arbitrary multiple charge distribution of the probe molecule.

The dielectric friction on the proteins has been calculated from the expression of Alavi and Waldeck for arbitrary multiple charge distribution model given below [30],

$$\zeta_{DF} = \frac{8}{R_c} \frac{\epsilon_s - 1}{(2\epsilon_1 + 1)^2} \tau_D \sum_{j=1}^N \sum_{i=1}^N \sum_{l=1}^{\infty} \sum_{m=1}^l \left(\frac{2l+1}{l+1} \right) \frac{(l-m)!}{(l+m)!} q_i q_j \left(\frac{r_i}{R_c} \right)^l \left(\frac{r_j}{R_c} \right)^l \times m^2 P_l^m(\cos \theta_i) P_l^m(\cos \theta_j) \cos(m\phi_{ji}) \quad (2)$$

where R_c is the cavity radius, (r_i, θ_i, ϕ_i) is the position vector and q_i is the partial charge of the i th atom. $P_l^m(\cos(\theta_i))$ is the Legendre polynomial. The maximum value of l used in the Legendre polynomial is 50. ϵ_s is the static dielectric constant of the solvent. Since the solvent here is water, ϵ_s is taken to be 78 and the Debye relaxation time τ_D is taken as 8.3 picosecond (ps).

The partial charges (q_i) of the atoms constituting the proteins have been calculated using the extended Huckel model of the semi empirical calculation package of Hyperchem software. The dielectric friction is calculated on each of the atoms in a protein. The rotational frictions around X, Y and Z direction are calculated by changing the labels of the atom coordinates. The average dielectric constant ζ_{DF}^{av} is the

harmonic mean of the dielectric frictions along X, Y and Z direction. Here X, Y, and Z denote the space fixed Cartesian coordinate of the proteins, as obtained from PDB [32].

Table 1 shows the values of dielectric friction along X, Y, Z direction and their average. Continuum calculation method of the dielectric friction formulated by Alavi and Waldeck is dependent on the cavity radius and has been discussed in detail by them [30]. They calculated the cavity radius from the observed orientational relaxation time of the organic molecules. The ratios of the longest bond vector of the organic molecules to the cavity radius ranged from 0.75 to 0.85. In Table 1, the calculations of dielectric friction are performed using the cavity radius such that the ratio of the longest bond vector to the cavity radius is 0.75.

In Table 2, we compared the average dielectric friction for the two above ratios – 0.75 (denoted as $\zeta_{DF}^{0.75}$) and 0.85 (denoted as $\zeta_{DF}^{0.85}$). $\zeta_{DF}^{0.85}$ is always larger than $\zeta_{DF}^{0.75}$ since the shorter cavity radius will put the charges close to the surface of the cavity, thereby increasing the polarization of the solvent and hence the rotational friction of the molecule.

2.2 Hydrodynamic Friction

The hydrodynamic rotational friction of the protein depends on its shape and size. Hydrodynamic friction was estimated earlier by the well-known DSE relation (Eq. 1). Perrin in 1936 [36] extended the DSE theory to calculate the hydrodynamic friction for molecules with prolate and oblate like shapes. Both prolate and oblate have two unequal axes. Harding [5] further extended the theory to calculate the hydrodynamic friction using a tri-axial ellipsoid. All the above theories employ stick binary condition to obtain the hydrodynamic friction.

Tri-axial ellipsoidal technique requires the construction of an equiv-

alent ellipsoid of the protein. We have followed the method of Taylor *et al.* to construct an equivalent ellipsoid from the moment matrix [37]. The eigenvalues of this equivalent ellipsoid are proportional to the square of the axes. So this method provides with the two axial ratios. We then obtained the values of the axes using the formula given by Mittelbach [38]

$$R_\gamma^2 = \frac{1}{5}(A^2 + B^2 + C^2) \quad (3)$$

R_γ is the radius of gyration and A , B and C are the three unequal axes of a particular protein.

Once the protein is represented as an ellipsoid with three principle axes, the hydrodynamic friction is calculated using Harding's method [5, 39]. The hydrodynamic rotational friction of the ellipsoidal axes A , B and C are denoted as ζ_A , ζ_B and ζ_C . The above rotational friction is obtained from the series of equations given below [39],

$$\begin{aligned} \zeta_0 &= 8\pi\eta ABC, \\ \zeta_A &= \zeta_0 \frac{2(B^2 + C^2)}{3ABC(B^2\alpha_2 + C^2\alpha_3)}, \\ \zeta_B &= \zeta_0 \frac{2(A^2 + C^2)}{3ABC(A^2\alpha_1 + C^2\alpha_3)}, \\ \zeta_C &= \zeta_0 \frac{2(A^2 + B^2)}{3ABC(A^2\alpha_1 + B^2\alpha_2)}, \\ \alpha_1 &= \int_0^\infty \frac{d\lambda}{(A^2 + \lambda)\Delta}, \\ \alpha_2 &= \int_0^\infty \frac{d\lambda}{(B^2 + \lambda)\Delta}, \\ \alpha_3 &= \int_0^\infty \frac{d\lambda}{(C^2 + \lambda)\Delta}, \\ \Delta &= \left[(A^2 + \lambda)(B^2 + \lambda)(C^2 + \lambda) \right]^{\frac{1}{2}} \end{aligned} \quad (4)$$

η is the viscosity of the solvent. We have calculated the average of tri-axial hydrodynamic friction by taking a harmonic mean of the friction along three different axes, as given below,

$$\frac{1}{\zeta_{TR}^{av}} = \frac{1}{3} \left[\frac{1}{\zeta_{TR}^A} + \frac{1}{\zeta_{TR}^B} + \frac{1}{\zeta_{TR}^C} \right] \quad (5)$$

The values of hydrodynamic friction, along three principle axes (A , B and C) of the ellipsoid and their mean, are tabulated in the Table 3. The A , B and C axes are not the same as the space fixed X, Y, Z Cartesian reference frame. Note that the values obtained from the tri-axial method are much lower than the experimental values. Here, we can talk about an important aspect of standard hydrodynamic approach – hydration layer. One finds that hydrodynamic values of rotational friction underestimate the rotational friction unless the effect of hydration layer is taken into account. However, the effect of hydration layer is usually incorporated in an *ad hoc* manner, by increasing the percentage of encapsulation of the atoms inside the ellipsoid [12, 11]. In this method, once the two axial ratios are obtained from the equivalent ellipsoid, the actual values of the axes are obtained by increasing the encapsulation of the protein atoms inside the ellipsoid. In the calculation presented here, the axes are obtained by equating with the radius of gyration. Therefore, we considered *no hydration layer* in this calculation of hydrodynamic friction. Later, we will show that this effect of hydration layer comes from the dielectric friction.

2.3 Total rotational friction: Comparison with experimental results

We define the total rotational friction as the sum of dielectric friction (ζ_{DF}^{av}) and the hydrodynamic friction without the hydration layer (i.e. tri-axial friction, ζ_{TR}^{av}) as given below,

$$\zeta_{total} = \zeta_{DF}^{av} + \zeta_{TR}^{av} \quad (6)$$

In Table 4, we have shown the values of the average dielectric (ζ_{DF}^{av}), hydrodynamic (ζ_{TR}^{av}) friction. Total friction (ζ_{total}) defined above is shown in the fourth column. To compare with the experimental results, we have shown the experimental values of the rotational friction in the next column. Note here, while the total friction, which is the contribution from both dielectric and hydrodynamic friction, is close to the experimental result, the microscopic bead modeling predicts the result, which is close to experimental value by itself [7]. The last column of Table 4 shows the references of the articles from which the experimental results are obtained.

The similarity between the total friction and the experimental friction is shown in figure 1, where we have plotted the experimental values of rotational friction against the total friction for a large number of proteins. For most of the proteins, the results fall on the diagonal line.

From the results shown in Table 4, we can conclude that the sum of dielectric friction and the hydrodynamic friction of the dry protein is approximately equal to the experimental results.

$$\zeta_{total} \approx \zeta_{exp} \tag{7}$$

3 Conclusion

Let us first summarize the main results of this work. We have calculated the hydrodynamic rotational friction on proteins using the tri-axial ellipsoid method, formulated by Harding [5], and the dielectric friction using the generalized charge distribution model derived by Alavi and Waldeck [30]. The hydrodynamic friction is calculated without the inclusion of any hydration layer. We have found that the combined effect of dielectric and hydrodynamic friction gives an estimate close to the experimental result. This approach seems to provide

a microscopic basis for the standard hydrodynamic approach, where a hydration layer is added to the protein in an *ad hoc* manner, to calculate rotational friction.

The calculations adopted here are still not without limitations. The continuum calculation of dielectric friction is dependent on the assumed cavity radius. Unfortunately, there is yet no microscopic basis to assume certain value of the cavity radius for the calculation of dielectric friction. Moreover, the effect of increasing dielectric constant of the solvent from the vicinity of the protein to the bulk is not taken into account by Alavi and Waldeck [30]. Thus, we have attempted to incorporate a multi shell model to incorporate multiple shells with varying dielectric constants. The theory is described in the appendix in detail. The drawback of incorporation of multiple shells in the continuum is that the frictional contributions from each of the shells add up, thereby giving rise to an unphysical large result.

Similarly, the tri-axial method and bead modeling method suffer from the lack of microscopic basis to determine the exact values of the axes and the bead size, respectively.

A potentially powerful approach to the problem is the mode coupling theory [40], which uses the time correlation formalism to obtain the memory kernel of the rotational friction. The total torque is separated into two parts – a short range part (which is called the bare friction Γ_{bare}) and a long range dipolar part. The advantage of mode coupling theory is that it does not depend on any parameter. It uses a time dependent effective potential field in terms of density distribution and the direct correlation function given by [40],

$$V_{eff}(\mathbf{r}, \Omega, t) = -k_B T \int dr' d\Omega' c(\mathbf{r} - \mathbf{r}', \Omega, \Omega') \nabla_{\Omega} \rho(r', \Omega', t) \quad (8)$$

The torque density is then expressed as,

$$\mathbf{N}_c(\mathbf{r}, \Omega, t) = n(\mathbf{r}, \Omega, t) \left[-\nabla_{\Omega} V_{eff}(\mathbf{r}, \Omega, t) \right] \quad (9)$$

where, $n(\mathbf{r}, \Omega, t)$ is the number density of the tagged particle. The rotational friction comes from the torque-torque correlation function.

The final expression of the single particle (Γ_s) and collective friction (Γ_c) are given by [41],

$$\Gamma_s(z) = \Gamma_{bare} + \mathcal{A} \int_0^\infty e^{-zt} \int_0^\infty dk k^2 \sum_{l_1 l_2 m} c_{l_1 l_2 m}^2(k) F_{l_2 m}(k, t) \quad (10)$$

$$\Gamma_c(z) = \Gamma_{bare} + \mathcal{A} \int_0^\infty e^{-zt} \int_0^\infty dk k^2 \sum_{l_1 l_2 m} F_{l_1 m}^s(k, t) c_{l_1 l_2 m}^2(k) F_{l_2 m}(k, t) \quad (11)$$

where, $\mathcal{A} = \frac{\rho}{2(2\pi)^4}$. $c_{l_1 l_2 m}$ is the $l_1 l_2 m$ -th coefficient of the two particle direct correlation function between any two dipolar molecules. $F_{l_1 l_2 m}^s$ and $F_{l_2 m}(k, t)$ are the single particle and the collective orientational correlation functions, respectively.

Eq. 10 and Eq. 11 are the standard mode coupling theory expressions for rotational friction. It has to be solved self consistently. In the overdamped limit, the self dynamic structure factor is expressed as,

$$F_{lm}^s(k, z) = \left[z + \frac{k_B T l(l+1)}{I \Gamma_s(z)} \right]^{-1} \quad (12)$$

and the collective dynamic structure factor is given by,

$$F_{lm}^c = F_{lm}(k) \left[z + \frac{k_B T f_{lm}(k) l(l+1)}{I \Gamma_c(z)} + \frac{k_B T k^2 f_{lm}(k)}{M \Gamma_T(z)} \right]^{-1} \quad (13)$$

where $f_{lm}(k) = 1 - (-1)^m (\rho/4\pi) c_{lm}(k)$. I and M are the moment of inertia and the mass of the dipolar molecule, respectively. $\Gamma_T(z)$ is the frequency dependent translational friction.

The advantage of the mode coupling approach is that the once the charge density of the protein molecules and the dipole density of the water molecules surrounding the protein are defined, the rotational friction can be obtained in terms of the direct correlation function and the static and dynamic structure factors of the protein-water systems. These are again related by Ornstein-Zernike equation [42].

The important aspect of this microscopic theory of dielectric friction is the hidden contribution of the translational modes. In the hydration layer, the rotational friction is enhanced due to the slow translational component. This effect of translation could not be approached through continuum calculation. Work in this direction is under progress.

4 Appendix : Multiple shell model and the Drawback

Dielectric constant of water varies from the vicinity of the protein to the bulk water value. To understand the effect of this varying dielectric constant on the rotational dielectric friction of the protein, we have performed the continuum calculation of rotational dielectric friction using a multiple shell model.

Nee and Zwanzig derived the dielectric friction contribution of a point dipole [27]. Alavi *et al.* [30] generalized it to obtain dielectric friction of a molecule with arbitrary distribution of charges. Castner *et al.* [43] generalized the point dipole approach to incorporate the discrete shell model with varying dielectric constant. Here, we have combined the approach of Castner *et al.* and Alavi *et al.* to obtain a generalized arbitrary charge distribution model for multiple hydration layers with varying dielectric constants around the protein. **Figure 2** shows the general scheme of this work. The protein is in the innermost cavity of radius a , where the water has a dielectric constant value of 4. The dielectric constant of water in the successive layers is assumed to increase up to the value of the bulk water, having a dielectric constant of 78. The width of each shell is assumed to be d .

We first write down the electrostatic potential in two dimensions, which could be generalized to three dimensions using principle of su-

perposition. The electrostatic potential $\Phi_j(\mathbf{r})$ can be written as,

$$\Phi_j(\mathbf{r}) = \Phi_j(r, \theta) = \sum_{l=0}^{\infty} B_l^j \frac{P_l(\cos \theta)}{r^{l+1}} + A_l^j r^l P_l(\cos \theta) \quad (14)$$

where, j denotes the number of concentric shells surrounding the protein. For n concentric shell, j can have a value from 0 to $n + 1$. $j = 0$ denotes no boundary. The boundary conditions are,

(i) $B_l^0 = q_i r_i^l$, where q_i and r_i are the partial charge and the position of the i th atom, respectively.

(ii) $\Phi \rightarrow 0$ as $r \rightarrow \infty$

(iii) $\Phi_j(r_j) = \Phi_{j+1}(r_{j+1})$, for $j = 0, 1, 2 \dots n$.

(iv) $\epsilon_j \Phi_j'(r_j) = \epsilon_{j+1} \Phi_{j+1}'(r_j)$, for $j = 0, 1, 2 \dots n$, $\Phi_j'(r) = \frac{\partial \Phi_j(r)}{\partial r}$.

(v) $A_l^{n+1} = 0$,

After incorporating the boundary conditions in Eq. 14, we get,

$$A_l^j = - \sum_{k=j}^n \frac{B_l^k}{r_k^{2l+1}} \times \left(\frac{\epsilon_{k+1}/\epsilon_k - 1}{\epsilon_{k+1}/\epsilon_k + \frac{l}{l+1}} \right) \quad (15)$$

where,

$$B_l^j = q_i r_i^l \left(\frac{2l+1}{l+1} \right)^j \prod_{k=1}^j \left(\frac{1}{\epsilon_k/\epsilon_{k-1} + \frac{l}{l+1}} \right) \quad (16)$$

The reaction potential is given by,

$$\Phi_j(r, \theta, \phi) = \sum_{i=1}^N \sum_{l=0}^{\infty} A_l^0 r^l P_l(\cos \gamma_i) \quad (17)$$

where,

$$P_l(\cos \gamma_i) = \frac{4\pi}{2l+1} \sum_{m=-l}^{m=l} Y_l^{m*}(\theta_i, \phi_i) Y_l^m(\theta_i, \phi_i) \quad (18)$$

After few steps of algebra, we obtain the frequency dependent dielectric friction given below,

$$\begin{aligned} \zeta_l^m(\omega) = & \sum_{j=1}^N \sum_{i=1}^N \sum_{l=1}^{\infty} \sum_{m=1}^l \frac{2q_i q_j}{a \omega} \left(\frac{r_i}{a} \right)^l \left(\frac{r_j}{a} \right)^l \times \\ & \frac{(l-m)!}{(l+m)!} P_l^m(\cos \theta_i) P_l^m(\cos \theta_j) m \cos(m \phi_{ji}) \times \end{aligned}$$

$$\sum_{s=0}^n \left| \text{Im} \left[\left(\frac{a}{a+sd} \right)^{2l+1} \left(\frac{\epsilon_{s+1,s}(m\omega) - 1}{\epsilon_{s+1,s}(m\omega) + \frac{l}{l+1}} \right) \times \right. \right. \\ \left. \left. \prod_{k=1}^s \left(1 - \frac{\epsilon_{k,k-1}(m\omega) - 1}{\epsilon_{k,k-1}(m\omega) + \frac{l}{l+1}} \right) \right] \right| \quad (19)$$

where, $\epsilon_{j,j-1} = \epsilon_j/\epsilon_{j-1}$, for all values of j . ϵ_0 is the dielectric constant of the cavity.

Above is the general expression of multiple (n) shell model. To write the final expression of dielectric friction for a two shell model, we assume Debye relaxation for the frequency dependent dielectric friction of two shells as given below,

$$\epsilon_{1,0}(m\omega) = 1 + \frac{\epsilon_{1,0} - 1}{1 + i m\omega \tau_{D1}} \quad (20)$$

$$\epsilon_{2,1}(m\omega) = 1 + \frac{\epsilon_{2,1} - 1}{1 + i m\omega \tau_{D2}} \quad (21)$$

where, τ_{D1} and τ_{D2} are the Debye relaxation time for the first and second shell.

The expression of dielectric friction for a two-shell model is given below,

$$\zeta_{DF} = \sum_{j=1}^N \sum_{i=1}^N \sum_{l=1}^{\infty} \sum_{m=1}^l \frac{8}{a} \left(\frac{2l+1}{l+1} \right) \frac{(l-m)!}{(l+m)!} q_i q_j \left(\frac{r_i}{a} \right)^l \left(\frac{r_j}{a} \right)^l \times \\ m^2 P_l^m(\cos \theta_i) P_l^m(\cos \theta_j) \cos(m\phi_{ji}) \times \\ \left[\frac{\epsilon_{1,0} - 1}{(2\epsilon_{1,0} + 1)^2} \tau_{D1} + \left(\frac{a}{a+d} \right)^{2l+1} \frac{\epsilon_{2,1} - 1}{(2\epsilon_{2,1} + 1)^2} \tau_{D2} \right. \\ \left. + 2 \left(\frac{a}{a+d} \right)^{2l+1} \frac{\epsilon_{1,0} - 1}{(2\epsilon_{1,0} + 1)^2} \frac{\epsilon_{2,1} - 1}{(2\epsilon_{2,1} + 1)^2} \times \right. \\ \left. \left\{ (2\epsilon_{1,0} + 1)\tau_{D2} + (2\epsilon_{2,1} + 1)\tau_{D1} \right\} \right], \quad (22)$$

The above expression has been numerically evaluated to find out the effect of dielectric friction on protein due to varying dielectric constant of water around the protein. The multiple shell model is found to overestimate the dielectric friction, as is evident from the above expression.

Acknowledgment The work is supported by DST, DBT and CSIR. A.M. thanks CSIR for Senior Research Fellowship.

References

- [1] G. Fleming, *Chemical Applications of Ultrafast Spectroscopy (monograph)*, (Oxford University Press, 1986).
- [2] E. H. Grant, *Dielectric behaviour of biological molecules in solution*, (Oxford University Press, 1978).
- [3] R. Pethig, *Dielectric and electronics properties of biological materials*, (John Wiley & Sons, 1979).
- [4] G. P. South and E. H. Grant, Proc. R. Soc. Lond. A. **328**, 371 (1972).
- [5] S. E. Harding, M. Dampier, and A. J. Rowe, IRCS Med. Sci. **7** 33 (1979).
- [6] J. G. de la Torre, Biophys. Chem. **93**, 159 (2001).
- [7] J. G. de la Torre, M. L. Huertas, and B. Carrasco, Biophys. J. **78**, 719 (2000).
- [8] B. Halle and M. Davidovic, Proc. Natl. Acad. Sci. (USA), **100**, 12135 (2003).
- [9] H-X. Zhou, Biophys. Chem. **93**, 171 (2001) *and references therein*.
- [10] B. Carrasco and J. G. de la Torre, Biophys. J. **75**, 3044 (1999).

- [11] S. E. Harding, *Biophys. Chem.* **93**, 87 (2001).
- [12] J. J. Muller, *Biopolymers*, **31**, 149 (1991).
- [13] S. Pal, S. Balasubramanian, and B. Bagchi, *J. Chem. Phys.* **117**, 2852 (2002).
- [14] M. M. Teeter, A. Yamano, B. Stec, and U. Mohanty, *Proc. Natl. Acad. Sci. U.S.A.* **98**, 11242 (2001) ; A. L. Tournier, J. Xu and J. C. Smith, *Biophys. J.* **85**, 1871 (2003).
- [15] S. Pal, J. Peon, B. Bagchi and A.H. Zewail, *J. Phys. Chem. B* **106**, 12376 (2002).
- [16] A. R. Bizzarri and S. Cannistraro, *J. Phys. Chem. B* **106**, 6617 (2002).
- [17] M. Marchi, F. Sterpone, and M. Ceccarrelli, *J. Am. Chem. Soc.* (2002).
- [18] R. Abseher, H. Schreiber, and O. Steinhauser, *Proteins* **25**, 366 (1996).
- [19] S. Balasubramanian and B. Bagchi, *J. Phys. Chem. B* **106**, 3668 (2002).
- [20] E. Dachwitz, F. Parak and M. Stockhausen, *Ber. Bunsen-Ges. Phys. Chem.*, **93**, 1454 (1989). S. Boresch, P. Höchtel, and O. Steinhauser, *J. Phys. Chem. B* **104**, 8743 (2000) ;
- [21] M. Cho, J. Y. Yu, T. Joo, Y. Nagasawa, S. A. Passino and G. R. Fleming, *J. Phys. Chem.*, **100**, 11944, (1996) ; S. Passino, Y. Nagasawa and G. R. Fleming, *J. Chem. Phys.*, **107**, 6094 (1997). N. Nandi and B. Bagchi, *J. Phys. Chem. A* **102**, 8217 (1998).
- [22] G. Otting, E. Liepinsh and K. Wüthrich, *Science*, **254**, 974 (1991). ; X. Cheng and B. P. Schoenborn, *J. Mol. Biol.* **220**, 381, (1991) ; V. A. Makarov, B. K. Andrews, P. E. Smith, and B. M. Pettitt, *Biophys. J.* **79**, 2966 (2000).

- [23] N. Nandi and B. Bagchi, J. Phys. Chem. **B** **101**, 10954 (1997).
- [24] B. Bagchi, Annu. Rep. Prog. Chem., Sect. C, **99**, 127 (2003).
- [25] J. A. Montgomery, Jr., B. J. Berne, P. G. Wolynes, and J. M. Deutch, J. Chem. Phys. **67**, 5971 (1977).
- [26] P. G. Wolynes, Phys. Rev. A **13**, 1235 (1976) ; S. Takada, J. Portman and P. G. Wolynes, Proc. Natl. Acad. Sci. **94**, 2318 (1997).
- [27] T-W. Nee and R. Zwanzig, J. Chem. Phys. **52**, 6353 (1970).
- [28] J. B. Hubbard and P. G. Wolynes, J. Chem. Phys. **69**, 998 (1978); ; B. Bagchi and G. V. Vijayadamodar, J. Chem. Phys. **98**, 3352 (1993) ; J. B. Hubbard, J. Chem. Phys. **69**, 1007 (1978).;
- [29] G. van der Zwan and J. T. Hvnes. J. Phvs. Chem. **89**,4181 (1985).
- [30] D. S. Alavi and D. H. Waldeck, J. Chem. Phys. **94**, 61196 (1991).
- [31] G. B. Dutt and T. K. Ghanty, J. Chem. Phys. **116**, 6687 (2002) ; *ibid* **115**, 10845 (2001) ; D. S. Alavi, R. S. Hartman, and D. H. Waldeck, J. Chem. Phys. **94** 4509, (1991).
- [32] H. M. Berman, J. Westbrook, Z. Feng, G. Gilliland, T. N. Bhat, H. Weissig, I. N. Shindyalov, P. E. Bourne, *Nucleic Acids Research* **28** 235 (2000)
- [33] B. U. Felderhof, Mol. Phys. **48**, 1269 (1983); *ibid* **48**, 1283 (1983); E. Nowak, J. Chem. Phys. **79** ,976 (1983).
- [34] P. G. Wolynes, Annu. Rev. Phys. Chem. 31,345 (1980)
- [35] P. Madden and D. Kivelson, J. Phys. Chem. **86**,4244 (1982).
- [36] F. Perrin, J. Phys. Rad. Ser. **VII** **5**, 497 (1934) ; *ibid* **7**, 1 (1936).

- [37] W. R. Taylor, J. M. Thornton, and W. G. Turnell, *J. Mol. Graph.* **1**, 30 (1983).
- [38] P. Mittelbach, *Acta. Phys. Austriaca.* **19** 53 (1964).
- [39] S. E. Harding, *Comp. Biol. Med.* **12**, 75 (1982); *ibid*, *Biophys. Chem.* **55**, 69 (1995) ;
- [40] B. Bagchi and A. Chandra, *Adv. Chem. Phys.* **80**, 1 (1991).
- [41] B. Bagchi , *J. Mol. Liq.* **77**, 177 (1998).
- [42] C. G. Gray and K. E. Gubbins, *Theory of Molecular Fluids*, (International Series of Monographs on Chemistry, Clarendon Press, Oxford, 1984).
- [43] E. W. Castner, Jr., G. R. Fleming, B. Bagchi, *J. Chem. Phys.* **89**, 3519 (1988).

Table 1

Table for the dielectric friction. The unit is 10^{-23} erg-sec. Cavity radius is chosen such a way that the ratio of longest bond vector (R_{max}) of the protein to the chosen cavity radius (R_C) is 0.75.

Molecule	R_C (Å)	ζ_{DF}^X	ζ_{DF}^Y	ζ_{DF}^Z	ζ_{DF}^{av}
6pti	29.50	17.8	13.2	18.1	16.0
1ig5	26.10	43.3	36.6	39.1	39.5
1ubq	34.30	18.1	18.3	21.8	19.3
351c	25.50	52.3	41.0	41.9	44.5
1pcs	27.20	90.5	51.3	66.1	65.7
1a1x	33.10	63.0	68.9	49.5	59.3
1gou	32.20	43.8	67.8	103.6	63.5
1aqp	35.30	44.5	71.1	132.1	68.0
1e5y	33.10	98.9	70.6	89.9	84.7
1bwi	35.70	78.3	60.5	108.1	77.8
1b8e	33.50	113.3	112.2	110.5	112.0
4ake	50.30	76.1	170.8	123.4	110.7
3rn3	35.00	118.8	89.0	56.8	80.5
1mbn	28.00	170.7	162.0	160.6	164.3

Table 2

Cavity size dependence of the dielectric friction. The unit is 10^{-23} erg-sec.

Molecule	$\zeta_{DF}^{0.75}$	$\zeta_{DF}^{0.85}$
6pti	16.4	25.7
1ig5	39.7	61.3
1ubq	19.4	30.3
351c	45.1	69.3
1pcs	69.3	111.0
1a1x	60.5	96.4
1gou	71.7	114.6
1aqp	82.6	132.3
1e5y	86.5	136.4
1bwi	82.3	128.9
1b8e	112.0	174.1
4ake	123.4	211.7
3rn3	88.2	138.1
1mbn	164.5	263.1
6lyz	107.8	172.7

Table 3

Table for the stick hydrodynamic friction using tri-axial ellipsoid. The unit is 10^{-23} erg-sec.

Molecule	R_γ (Å)	ζ_{TR}^A	ζ_{TR}^B	ζ_{TR}^C	ζ_{TR}^{av}
6pti	11.34	57.8	83.4	85.1	73.1
1ig5	11.36	72.9	78.9	84.9	78.6
1ubq	11.73	71.2	89.9	94.0	83.8
351c	11.51	77.3	84.5	85.3	82.2
1pcs	12.38	78.9	106.5	111.3	96.6
1a1x	13.47	120.8	127.3	143.8	129.9
1gou	13.61	103.3	141.7	148.2	127.7
1aqp	14.45	117.7	171.1	177.0	150.1
1e5y	13.81	108.9	145.7	155.3	133.4
1bwi	13.94	106.9	155.4	158.2	135.7
1b8e	14.70	167.5	172.5	178.2	172.6
4ake	19.59	298.3	422.7	442.8	376.1
3rn3	14.31	112.9	166.5	172.2	145.1
1mbn	15.25	163.7	181.2	210.1	183.1

Table 4

Comparison between the total friction and the experimental results. Results are given in the unit of 10^{-23} erg-sec. The references to the experimental results of rotational diffusion of the corresponding proteins are given in the Ref. [8] .

Protein	PDB id	ζ_{DF}^{av}	ζ_{TR}^{av}	ζ_{total}	ζ_{exp}
Bovine pancreatic trypsin inhibitor	6pti	16.0	73.1	89.1	96.8
Calbindin D9k, holo form	1ig5	39.5	78.6	118.1	125.0
Human ubiquitin	1ubq	19.3	83.8	103.1	118.9
Ferricytochrome c_{551}	351c	44.5	82.2	126.7	130.1
Plastocyanin, Cu(II) form	1pcs	65.7	96.6	162.3	149.5
Oncogenic protein p13 ^{MTCP1}	1a1x	59.3	129.9	189.2	241.9
Binase	1gou	63.5	127.7	191.2	191.3
Ribonuclease A	1aqp	68.0	150.1	218.1	186.1
Azurin, Cu(I) form	1e5y	84.7	133.4	218.1	190.4
Hen egg-white lysozyme	1bwi	77.8	135.7	213.5	203.6
Bovine -lactoglobulin, monomer	1b8e	112.0	172.6	284.6	270.6
Adenylate kinase, apo form	4ake	110.7	376.1	486.8	478.2
Bovine Ribonuclease A	3rn3	80.5	145.1	225.6	235.0
Sperm Whale Myoglobin	1mbn	164.3	183.1	347.4	246.3

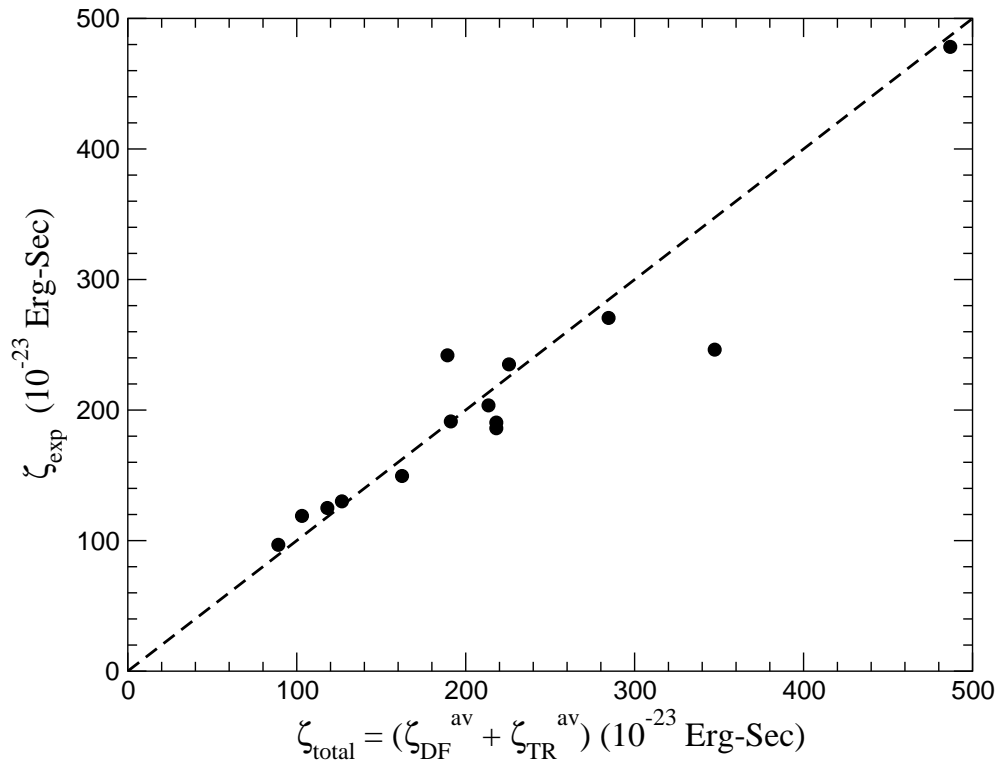


Figure 1: The combined friction from hydrodynamic and dielectric is plotted against the experimental results. The solid line shows the diagonal to guide the eye.

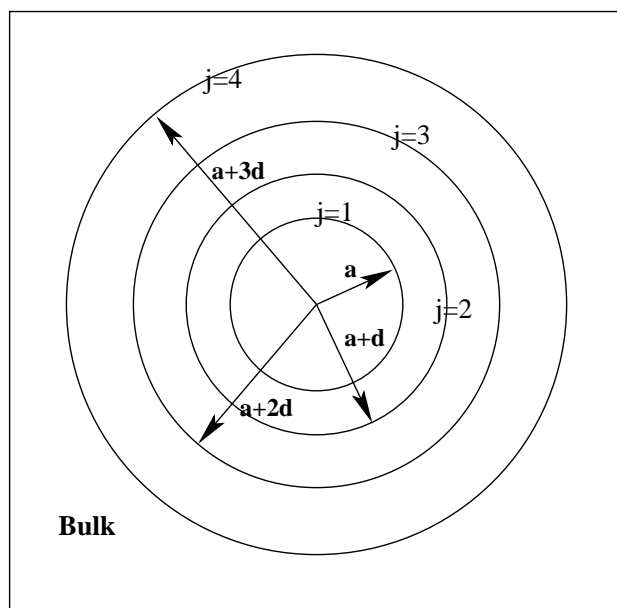


Figure 2: schematic diagram of the Molecular cavity and the hydration shell constituted by the bound water molecules. The bulk water molecules are more randomly oriented